The 14th World Conference on Earthquake Engineering
October 12-17, 2008, Beijing, China

LOAD HISTORY EFFECTS ON DEFORMATION CAPACITY OF FLEXURAL MEMBERS LIMITED BY BAR BUCKLING

D. V. Syntzirma[1], S. J. Pantazopoulou[2] and M. Aschheim[3]

[1] *Civil Engineer, MSc, PhD Candidate, Dept. of Civil Eng., Demokritus University of Thrace, Xanthi, Greece*
[2] *Professor, Depart. of Civil Engineering, Demokritus Univ. of Thrace, Xanthi, Greece*
[3] *Associate Professor, Depart. of Civil Engineering, Santa Clara Univ., Santa Clara, U.S.A.*
Email: dsyntz@civil.duth.gr, pantaz@civil.duth.gr, maschheim@scu.edu

ABSTRACT :

Post earthquake reconnaissance reports illustrate that failure of reinforced concrete (R.C.) members often involve buckling of reinforcement, an observation suggesting that this phenomena is prerequisite for the necessary reduction of member length (shortening) that marks failure under transverse cyclic displacement reversals. From previous experimental research it is known that occurrence of buckling is linked to displacement history. In the present paper the problem of bar buckling in the plastic hinge region as a limiting factor of deformation capacity of reinforced concrete members is expressed, using as a vehicle the hysteretic stress−strain model of the reinforcement, in terms of the imposed displacement amplitude under cyclic reversals. Through the derived analytical expressions it is shown that when controlled by bar buckling, deformation capacity cannot be defined uniquely as it varies with the path of applied load. This explains in part the wide scatter of experimental results regarding drift capacity, which is particularly intense in cases where premature modes of failure are suppressed and the response is controlled by flexure. A corollary to this finding, which refers to the established procedures of displacement−based design, is that quantifiable indices of deformation capacity, associated with the various failure modes, need be expressed as lower bounds, to reflect the wide range of expected values as these might be limited by the occurrence of buckling of compression reinforcement under realistic earthquakes.

KEYWORDS: bar buckling, rotation capacity, ductility, reinforcement, deformation, instability, failure

1. INTRODUCTION

A point of contention in modern displacement−based earthquake design or assessment approaches for reinforced concrete structures is the ability to obtain dependable estimates of deformation capacity of the individual structural members under lateral sway. Deformation capacity refers to the drift amount (i.e. member rotation from its respective chord, which is defined as the relative lateral displacement of the member's ends, divided by the member length), at the point of irrecoverable loss of lateral load resistance. To this end, a variety of experiments have been conducted, primarily on reinforced concrete columns, beams and walls, under pseudo−static cyclic displacement reversals simulating earthquake effects. The international database of tests has formed the basis for calibration of empirical, semi−empirical, or even mechanistic models of deformation capacity (e.g. Pantazopoulou 2003 and references thereof). Such are needed as acceptance criteria, i.e., to check adequacy of the individual members of the structure against the deformation demands imposed by the design earthquake. There are a number of issues in this approach, as follows:

(a) The database of published tests is marked by excessive scatter indicating that drift capacity depends on a large number of different factors not adequately reflected in the design expressions (Pantazopoulou 2003, Syntzirma and Pantazopoulou 2002). The scatter is not eliminated by separation of the tests in groups depending on the mode of failure (shear, lap−splice/anchorage, or flexure−shear), or when the sensitivity to relevant design parameters such as longitudinal, transverse reinforcement ratio, and axial load ratio is explicitly accounted for, by further calibration of the design expressions against groups of tests (Inel et al 2004, Zhu et al 2006). In general, drift capacity is small (ductility in the range of 0.5−2.5) for members underdesigned in shear or with inadequate splices/anchorages. The paradox is that the scatter in dependable ductility is much greater when premature failures of this type are unlikely and flexural failure response prevails even after degradation owing to cycling.

(b) A significant point of difference between individual investigations contributing to the database lies in the displacement history used to simulate the earthquake effect. It is common to conduct the tests by applying a sequence of symmetric displacement cycles so as to induce combined flexure−shear in the tested element. Usually either 1, 2 or 3 cycles at each displacement level are applied prior to proceeding to a higher displacement magnitude, the increments between levels being expressed in fractions of the yield displacement of the member (e.g. a typical history is three cycles at ductility levels of 0.5, 1.0, 1.5, 2.0, 2.5, 3.0, 3.5, 4.0). The number of cycles at each level, but most importantly the step used in the incremental sequence, both have a great influence in the recorded response. Note that the step by which lateral displacement is increased from level to level quantifies the maximum strain difference inflicted upon a reinforcing bar (i.e. it represents the breadth of a hysteresis loop) between extremes of response within a single cycle. Thus, it quantifies the magnitude of residual tensile strain upon unloading from tension, and therefore the amount of drift that need be imposed in the reversed direction prior to closure of the cracks crossed by the same bar when in compression. Considering that in simulated earthquake tests buckling of rebars is always sideways, and a determining parameter is the tangent stiffness of the bar as it follows its hysteretic stress−strain response, it follows that the displacement step increment of the imposed load history affects significantly occurrence of sideways instability.

The uncertainty associated with the displacement history on buckling is even more relevant when considering the inherently asymmetric nature of near field earthquake records which are marked by few large pulses rather than an incremental symmetric increase of amplitude as would be implied by the simulated pseudo−static tests.

2. DEFINITION OF ROTATION CAPACITY AT BAR BUCKLING

To interpret the experimental facts outlined in the preceding, the formal definition of flexural rotation capacity in a reinforced concrete member under lateral sway is considered in the remainder of this paper: drift at failure, q_u is the least of the values $q_{cc,u}$, $q_{st,u}$ and $q_{sc,u}$, which represent the theoretical estimates of member rotation (measured with respect to its chord) at concrete compression failure, tension reinforcement rupture, and occurrence of theoretical buckling conditions of compression reinforcement. The basic model in the discussion that follows is that of cantilever under a transverse shear force at the tip point, since the statics of this problem are identical to those of half the span in a regular frame member under lateral sway (the length of the cantilever model, L_s, is equal to half the span of the reference member, whereas all other section properties are identical to those at the end supports of the frame element). In general, the flexural component of drift associated with any particular material strain value at the member's critical section (here for example, compression reinf. buckling), follows the familiar procedure of integration of curvatures along the member length:

$$q^f = q_p^f + q_y^f = f_{sc,u} \cdot \boldsymbol{l}_p + \frac{1}{3} f_y \cdot (L_s - \boldsymbol{l}_p) \qquad (2.1)$$

Superscript f marks the flexural origin of the estimated drift components (to distinguish from terms owing to reinforcement slippage, shear deformations, etc.), $f_{sc,u}$ is the curvature of the critical cross section upon attainment of bar buckling, f_y is the yield curvature, and $\boldsymbol{l}_p$ is the length of the plastic hinge. For clockwise positive rotation, the curvature terms in Eqn. (2.1) are defined by:

$$f_{sc,u} = -\frac{e_{sc,u}}{c_u - d'}; \quad f_y = min\left\{\left(e_{sy} + \frac{s_y}{d}\right)\cdot\frac{1}{d - c_y}; \quad -\frac{0.75 e_{c,o}}{c_y}\right\} \qquad (2.2)$$

where, $e_{sc,u}$ is the critical axial compression strain upon attainment of instability conditions for the longitudinal compression reinforcement (compression negative), c_u is the depth of the compression zone of the member's cross section at the ultimate (for a constant axial load, c_u is very close to the corresponding value c_y at tension reinf. yielding), d' is the concrete cover to the centroid of compression reinforcement. Sign convention in this paper is compression negative. Bar slip from its end anchorage causes a lumped rotation at the face of the support, defined here as q^s. Usually the total drift magnitude is obtained as the sum of the flexural and slip contributions without any interaction between the two. However, the lumped rotation at the support causes a local increase in the axial strain of the compression zone, which in turn affects equilibrium of forces in the cross section, and the magnitude of curvature, f. A general equation relating axial compressive strain at a distance y from the neutral

axis of the cross section, $e_c(y)$, with slip s of tension reinforcement is (Fig. 1):

$$e_c(y) = -\left(e_s + \frac{s}{d}\right)\cdot\frac{y}{d-c} \qquad (2.3a)$$

Here it was assumed that the effect of additional compression strain owing to slip attenuates linearly to a distance equal to d from the support of the member (i.e., the denominator d in the s/d component in Eqn. (2.3a)). The term s_y/d accounts for the additional axial strain generated in the compression zone of the member as a result of the tension bar pullout, s_y, at the onset of bar yielding. The theoretical definition for $q_{sc,u}$ at bar buckling is expressed in terms of the critical strain as:

$$q_{sc,u} = q^f_{sc,u} + q^s_{sc,u} = -\left(\frac{e_{cc,u}}{c_u - d'}\right)\cdot \mathbf{l}_p + \frac{1}{3} f_y \cdot (L_s - \mathbf{l}_p) + q^s_{sc,u} \qquad (2.3b)$$

where, $e_{cc,u}$ is the concrete strain at the location of the compression reinforcement when the latter reaches its critical buckling strain, $e_{sc,u}$ and $q^{\,s}_{sc,u}$ is the drift component owing to pullout of tension reinforcement at the onset of bar buckling, i.e.:

$$q^s_{sc,u} = \frac{s_u}{d - c_u}; \quad \text{where,} \quad s_u = s_y + (e_{su} - e_{sy})\frac{f_{su} - f_{sy}}{f_{b,u}}\cdot\frac{D_b}{4} \qquad (2.3c)$$

where, f_{su} is the ultimate strength of the bar, f_{sy} is the yield stress, D_b is the bar diameter, and $f_{b,u}$ is the average bond strength that the anchorage may support at attainment of bar strength (here this is assumed to be 80% of the design value). Note that concrete compression strain rather than bar strain was used here to define curvature (to avoid the uncertainty in bar strain values which are affected by cycling). Critical conditions in the reinforcement may not be followed by catastrophic buckling if an alternative state of equilibrium can be produced in the cross section, resulting from redistribution of the compressive forces from the unstable compression steel to the concrete core. This is not possible in lightly confined R.C. members (representative of older detailing practices), in members with a prominent flexural action (low axial load), or under reversed cyclic load where cracks remain open. In such cases attainment of the critical compression strain in the longitudinal reinforcement corresponds to buckling failure and the theoretical estimate for $q_{sc,u}$ defines the critical rotation capacity of the member.

3. CRITICAL BUCKLING STRAIN, $e_{sc,u}$, UNDER MONOTONIC LOAD

From Eqn. (2.3b) it follows that the true unknown of the problem is the axial strain of compression reinforcement, $e_{sc,u}$, when it reaches critical conditions, as well as its relationship with the compression strain in the concrete at the same distance from the neutral axis of the cross section, $e_{cc,u}$. The same problem under monotonic (as opposed to cyclic) strain conditions is already solved: a bar segment supported by two successive stirrups (i.e. assuming that the unsupported length is equal to the spacing of successive ties S_{st}), under axial compression will buckle sideways at a postyielding stress f_s, when (Syntzirma and Pantazopoulou 2006):

$$S_{st}/D_b = 0.785\sqrt{E_s/f_s}\ ; \quad E_s = 200\,GPa, \text{ if } e_s < 0,\ |e_s| \le e_{sy}; \quad E_s = E_r, \quad \text{if } e_s < 0,\ |e_s| > e_{sy} \qquad (3.1)$$

In Eqn. (3.1) E_r is the double modulus value which is a weighted average between the tangent stiffness of the bar, E_t, and the initial elastic modulus E_s, to account for the elastic unloading of the tension side of the buckling bar as it bends (Papia et al 1988). (Ratio E_r/E_s, is plotted against the ratio E_t/E_s in Fig. 5 in (Pantazopoulou 1998)). For a given value of tie spacing (provided S_{st} suffices to prevent elastic buckling of the main bars), the dependable axial compressive strain at which reinforcement is likely to buckle, $e_{sc,u}$, is calculated from Eqn. (3.1), and clearly depends upon the strain hardening characteristics of compression steel. The resulting relationship between the strain ductility ratio of compression reinforcement, $me_{sc,u}=e_{sc,u}/e_{sy}$ and the spacing of stirrups normalized with respect to the bar diameter D_b has the form of an interaction diagram, which is a characteristic of the reinforcement uniquely defined by its post−yielding hardening properties (Fig. 2(a)). The lower right−hand range of the diagram is controlled by the characteristics of the stress−strain response of the reinforcement at the onset of strain hardening; the above relationships break down if E_t=0. Bar strains within the yield plateau are below the interaction diagram and can only be sustained without failure if the member concrete core is sufficiently confined (Fig. 2(a)). Thus, the present analysis is meaningful if the axial strain capacity of the confined core calculated

from pertinent confinement models (e.g. Pantazopoulou 2003) exceeds the strain at the onset of strain hardening of the reinforcement. This restriction is consistent with the scope of the study, i.e., member failures dominated by flexure.

Under reversed cyclic loading, the actual bar strain follows the hysteretic stress−strain behavior of the reinforcement, as required by the imposed displacement history. To establish a characteristic interaction diagram for that problem in a manner analogous to what the monotonic case described above, it is necessary to refer to a hysteretic stress−strain model of reinforcement behavior under reversed axial load, and a strain–displacement relationship, so that given the displacement history imposed on the member, a strain ductility demand may be established for the compression steel.

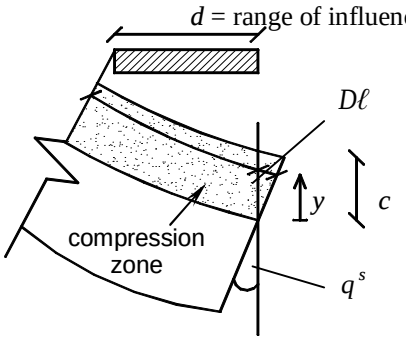

$$D\ell(y) = s \cdot \frac{y}{d-c}$$

$D\ell$: fiber−shortening due to slip

$$De_c = \frac{\Delta \mathbf{l}(y)}{d} = \frac{s}{d} \cdot \frac{y}{d-c}$$

Figure 1 Additional Compressive Strain caused by Bar Pullout in the Tension Zone

4. HYSTERETIC RESPONSE OF REINFORCING STEEL

A hysteretic relationship enables calculation on the bar axial stress f_s, given the axial strain, by systematically following through the load history. Apart from the monotonic envelope in tension and compression, which bounds cyclic response, a general expression for the branch curve that describes the path of transition from one envelope curve to the other (i.e. from tension to compression and vice−versa) is necessary. The complete hysteretic stress−strain model used in the present study is depicted in Fig. 2(b), 2(c) and is described by the following expressions:

(a) Envelope Curve for Response in Tension and Compression:

$$f_s^{env} = E_s \cdot e_s \quad \text{for } e_s \le e_{sy}\ , \quad f_s^{env} = f_{sy} \quad \text{for } e_{sy} \le e_s < e_{sh} \tag{4.1a}$$

$$f_s^{env} = \frac{f_{sy} - f_{su}}{e_{sh} - e_{su}} \cdot (e_s - e_{sh}) + f_{sy} \quad \text{for} \quad e_{sh} < e_s \le e_{su} \tag{4.1b}$$

where, f_s^{env} is the envelope stress, e_s is the total bar axial strain, f_{sy} and e_{sy} are the characteristic yield stress and strain of the reinforcement, e_{sh} is the reinforcement strain at the onset of strain hardening, and f_{su} and e_{su} are the corresponding values at the point of tensile rupture (Fig. 2(b)).

(b) Branch Curve (Hysteresis Loops): (modified Menegotto−Pinto model) The stress is defined as:

$$f_s = f_s^Q + f_s^* \cdot (f_s^P - f_s^Q) \quad \text{where,} \quad f_s^* = \left[\frac{1-b}{\left(1 + (e_s^*)^R\right)^{1/R}} + b \right] \cdot e_s^* \quad \text{and} \quad e_s^* = \frac{\left| e_s - e_s^Q \right|}{\left| e_s^P - e_s^Q \right|} \tag{4.2}$$

Terms e_s^Q and f_s^Q are the strain and stress at the beginning of the branch curve; initial unloading from the envelope curve occurs along a line parallel to the elastic response. The end point of the linear unloading segment is the starting point of the branch curve, marked by letter Q in Fig. 2(b). As observed in steel coupon tests under reversed cyclic axial load, a distinct point of yielding occurs only once in the stress−strain response of steel. From that point on, transition from the tension to the compression regime (or vice−versa) follows along a branch curve that demonstrates a smooth knee at the point of theoretical yielding, tending asymptotically to the envelope curve with a slope $E_t = b \cdot E_s$.

In the present model, R is the radius of curvature of the branch curve at the point of theoretical yielding (marked by P in Fig. 2(b)), whereas e_s^P and f_s^P are the coordinates of that point in the stress−strain diagram (thus, in the model, theoretical yielding is defined along the linear elastic unloading curve, measured with reference to point Q). The tangent stiffness of the bar along the branch curve is given by:

$$E_t = \left[\frac{(1-b)}{\left(1+(e_s^*)^R\right)^{\frac{1+R}{R}}} + b \right] \cdot E_s \; ; \quad \text{where} \quad b = \frac{f_{su} - f_{sy}}{e_{su} - e_{sy}} \cdot \frac{1}{E_s} \tag{4.3}$$

The physical significance of all variables is illustrated in Fig. 2(b). Of those, coordinates of point Q and appropriate values for R and b have been obtained from calibration of the model with experimental results. For a given bar strain history, the complete stress−strain relation of a reinforcing bar is reproduced with the model using the following rules: (1) Linear stress−strain response up to first yielding in either direction. (2) Linear strain−hardening after yielding, up to strain reversal, which begins at a strain magnitude of e_s=e_{sr}^{env}, and a corresponding envelope stress, f_{sr}^{env}. A yield plateau only occurs once, in the first cycle; for the remainder of the loading cycles the envelope curve becomes bilinear. (3) Unloading from the envelope curve follows a linear line with a slope of E_s, down to point Q, i.e., to a strain of $e_s^Q = e_{sr}^{env} - e_{sy}$, and a corresponding stress $f_s^Q = f_{sr}^{env} - f_{sy}$. (4) Thereafter, the unloading curve displays a nonlinear hysteretic behavior that is described by Eqns. 4.2. (5) Identical procedure is followed when steel reverses from compression into tension. For these cases the milestone points for definition of the branch curve are Q' ($e_s^{Q'}$, $f_s^{Q'}$) and P' ($e_s^{P'}$, $f_s^{P'}$) as shown in Fig. 2(b).

To also account for degradation of the hysteretic properties with increasing applied bar strain, e_{sr}^{env}, R and b are taken to decay from the original values, R_o=1.6 and b_o (as per Eqn. (4.3)) according with:

$$\begin{aligned} R &= R_o \cdot k(e_{sr}^{env}) \\ b &= b_o \cdot k(e_{sr}^{env}) \end{aligned} \qquad k = 1.0; \text{ for } e_{sr}^{env} \le e_{sh} \text{ and } k = 1 - 0.5\frac{e_{sr}^{env} - e_{sh}}{e_{su} - e_{sh}} \text{ for } e_{sr}^{env} > e_{sh} \tag{4.4}$$

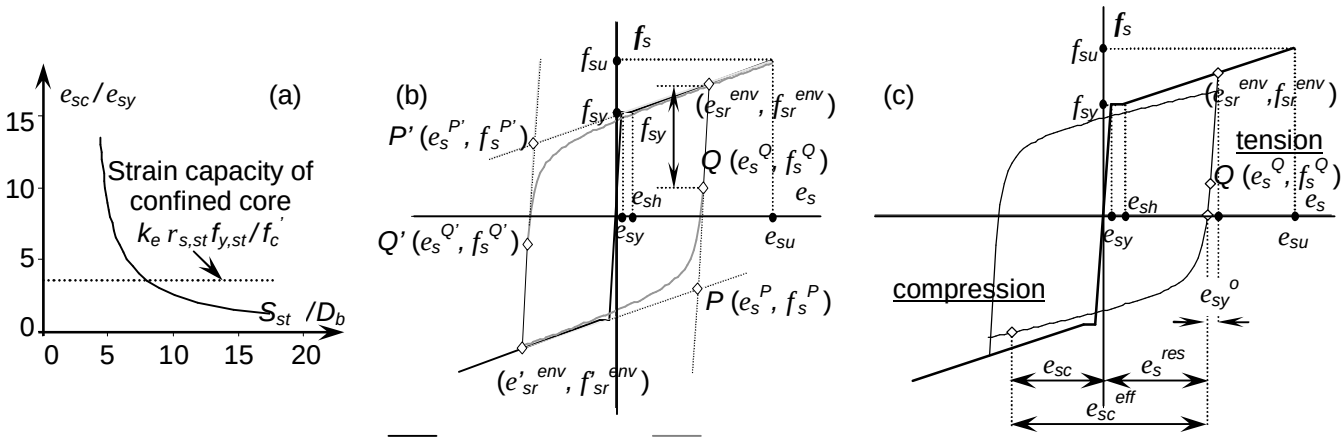

Figure 2 **(a)** Buckling Interaction Diagram showing Critical Strain versus S_{st}/D_b; **(b)** Basic Model for the Hyst. Stress−Strain Law of Rebar; **(c)** Definition of Actual Strain e_{sc}, and Effective Strain e_{sc}^{eff}

5. INTERACTION DIAGRAM FOR BAR BUCKLING UNDER CYCLIC LOAD

The basic buckling Eqn. (3.1) was derived from equilibrium and is generally valid. To formulate an interaction chart for cyclic strain history, which would relate the S_{st}/D_b ratio with the dependable compression strain ductility prior to attainment of instability conditions of the compression reinforcement Eqn. (3.1) is used. Here note the difference in the meaning of the critical compression strain under monotonic and cyclic conditions: in the monotonic case, the compression strain $e_{sc,u}$ is the actual strain value measured with reference to the zero point in the stress−strain diagram of the reinforcement. In the reversed cyclic stress−strain curve of the bar, the critical compression strain is measured with reference to the point of zero stress at any hysteretic branch curve unloading from tension into compression. This strain, denoted as $e_{sc,u}^{eff}$, is referred to as effective strain to distinguish from the actual bar strain which under certain loading conditions may be tensile (Fig. 2(c)).

Clearly, with reference to the hysteretic model it follows that conditions for bar buckling may occur in many different ways depending on the overall circumstances of the compression zone of the member and the imposed reinforcement strain history. Generally owing to the poor tensile behavior of concrete, strains sustained by the reinforcement in tension exceed the compression strains sustained by the same bars upon load reversal. Thus, the bars are more likely to first yield in tension thereby developing high residual tensile strains. Whether cracks remain open or are closed upon reversal of the load depends on the amount of maximum tensile strain, e_{sr}^{env}, sustained by the bar prior to unloading from the tension into the compression regime during the previous excursion (Fig. 2(c)).

Figure 3a plots the result of Eqn. (3.1) for a compressed reinforcing bar having the following stress−strain characteristics: 400 MPa yield strength (e_{sy}= 0.002), a yield plateau extending to a strain of e_{sh}= 0.005, and an ultimate strength of 600 MPa attained at a strain of e_{su}= 0.05. Results are obtained for different values of the unloading tension strain e_{sr}^{env} (in the plot, e_{sr}^{env} is taken equal to 0.003; 0.006; 0.010; 0.020; 0.030; 0.040 and 0.050); the *y* axis plots the effective bar strain at critical conditions, $e_{sc,u}^{eff}$, normalized with respect to the nominal yield strain value, e_{sy}; thus, it represents a strain ductility measure for the bar in compression. Note that the effective strain is measured with reference to the point of intersection of the unloading branch with the strain axis (Fig. 2(c)); thus through this calculation an interaction diagram is obtained, relating *effective* strain ductility with the S_{st}/D_b ratio at critical conditions. Since it mainly depends on the strain−hardening properties, this plot is in principle identical to that of monotonic behavior, after modifications to account for the reduced *b* value according to Eqn. (4.5). Thus, for each value of tension strain where unloading starts (e_{sr}^{env}), the resulting interaction curve is mildly modified from the previous one, owing to the influence of e_{sr}^{env} on *R* and *b*.

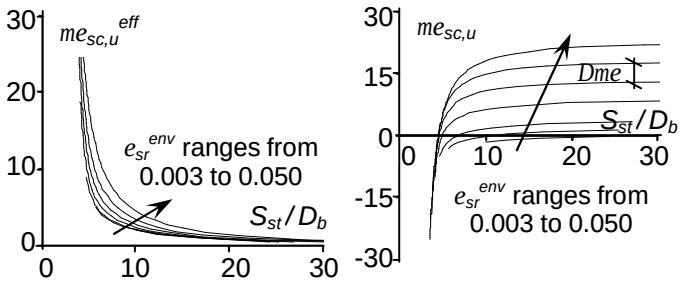

Figure 3 **(a)** Interaction Diagram for $me_{sc,u}^{eff}$ vs. S_{st}/D_b; **(b)** Interaction Diagram for $me_{sc,u}$ vs. S_{st}/D_b

The actual bar strain, $e_{sc,u}$, at attainment of critical conditions, is related to its effective strain counterpart, $e_{sc,u}^{eff}$, through the following relationship (Fig. 2(c)), where, $e_{sr}^{env}>0$ and the bar is unloaded from the tension envelope:

$$e_{sc,u} = e_s^{res} - e_{sc,u}^{eff} = e_{sr}^{env} - e_{sy}^{o} - e_{sc,u}^{eff} \tag{5.1a}$$

In strain ductility terms, Eqn. (5.1a) is expressed as follows:

$$me_{sc,u} = \frac{e_{sc,u}}{e_{sy}} = \frac{e_{sr}^{env} - e_{sy}^{o} - e_{sc,u}^{eff}}{e_{sy}} \approx me_{sr}^{env} - me_{sc,u}^{eff} - z \tag{5.1b}$$

In Eqn. (5.1b) *z* is an arithmetic constant ranging between 1.0 and 2.3, for a compressed reinforcing bar having the stress−strain characteristics considered in the preceding. Term $e_s^{res} = e_{sr}^{env} - e_{sy}^{o}$ represents the strain coordinate at the point of intersection of the branch curve with the strain axis, i.e., it is actually the residual tensile strain of the bar upon unloading from the tension envelope (Fig. 2(c)). In absolute value parameter e_{sy}^{o} is larger than e_{sy}, the difference increasing with the magnitude of e_{sr}^{env}. In deriving Eqn. (5.1b) the two quantities were related through the following expression which was obtained by fitting the exact values:

$$z = 0{,}0027 \cdot \left(me_{sr}^{env}\right)^2 - 0{,}0199 \cdot me_{sr}^{env} + 1{,}0792 \tag{5.2}$$

Thus, the critical buckling strain of the compression reinforcement not only depends on the constitutive properties of its branch and envelope curves (as reflected by the effective critical buckling strain), but it also depends on the magnitude of tensile strain sustained by the bar in its previous excursion into tension. This point conclusively demonstrates that conditions for bar buckling in R.C. members undergoing cyclic flexure/shear

reversals is not unique but rather, it is a function of the loading history. Dependence on displacement history is also valid when considering the corresponding drift or displacement ductility values associated with the onset of buckling. This result is plotted in Fig. 3(b) in the form of interaction diagrams between the true compression strain ductility of the reinforcement and the S_{st}/D_b ratio for several different levels of maximum attained tensile strain, e_{sr}^{env}. Curves are very similar in shape, but are shifted in the strain ductility axis by an amount *Dme*, which is equal to the normalized residual tensile strain magnitude, (e_s^{res}/e_{sy}). Note that the actual strain at critical (buckling) conditions is tensile except for very low magnitudes of sustained e_{sr}^{env} values (Fig. 3(b)). Thus, under reversed cyclic loading, compression bar buckling will generally occur with the bar carrying a compressive stress while being deformed by a significant amount of residual tensile axial strain. This residual bar strain at attainment of buckling conditions is higher (i.e. more tensile) the greater the value of maximum sustained tensile strain in the previous cycles.

Figure 4(a) plots for different S_{st}/D_b ratios the estimated strain at critical conditions, $e_{sc,u}$, against the peak strain attained on the tensile envelope during the previous cycle e_{sr}^{env}. Both variables are normalized with respect to the yield strain of the reinforcement, so that they actually represent strain ductility measures. The relationship is almost linear in the range of small e_{sr}^{env} values, becoming mildly nonlinear for higher strains. Note the effect of the S_{st}/D_b ratio on this relationship: for values greater than 5.5 (which is the range of practical interest) the critical buckling strain becomes increasingly tensile for any given level of e_{sr}^{env} as the stirrup to bar diameter ratio increases, whereas the reverse effect is observed on the effective strain (Fig. 4(b)). Thus, larger stirrup spacing leads to a larger value of actual tensile strain upon bar buckling. The effect of the loading history is highlighted by each curve, which may be considered a bound for the onset of instability: higher tensile strains attained by the reinforcement in the previous cycle cause buckling to occur at larger residual tensile strains upon load reversal. Note that each loading history, usually expressed in terms of displacement reversals, corresponds to a specific relationship between strains in the extreme tension and compression layers of reinforcement.

6. IMPLEMENTATION WITH EXPERIMENTAL RESULTS

The above procedure is used to interpret available experimental data. A prismatic cantilever column specimen is examined with shear span equal to 900mm, a cross section of 200mm square, reinforced with 4 corner 12mm diameter bars (f_{sy}=500MPa, f_{su}=700MPa, f_c'=20 MPa), having 6mm diameter perimeter stirrups ($f_{y,st}$=220 MPa) spaced at 6D_b (Specimen 7b in Syntzirma et al 2006). The column was tested under constant axial load (8% $f_c'A_g$) and a reversed cyclic lateral force applied at the tip through displacement control following a symmetric displacement history of increasing amplitude (Fig. 5(a)). The plot in Fig. 5(b) depicts strains in the top and bottom reinforcing layers as a function of imposed displacement ductility, as well as the peak points on the response load−drift curve (Fig. 5(a)). Also marked on the plots is the point of buckling failure. Evidently the nominal strains in both layers become increasingly tensile as the displacement amplitude is increased, but buckling will only take place when the strain history produces a lower magnitude strain in the compressed layer than the $e_{sc,u}$ value associated with the peak tensile strain attained in the previous step. Thus, at each loading cycle, which strains the reinforcement from an extreme tension strain of e_{sr}^{env}, to an extreme strain of e_{sc} upon displacement reversal, there are two possibilities regarding failure by bar instability (Fig. 5(c)):

(1) either $e_{sc} > e_{sc,u}$ (algebraically greater) and therefore, buckling will not occur during this displacement cycle
(2) $e_{sc} \le e_{sc,u}$, thus buckling will occur prior to attainment of the targeted strain magnitude, e_{sc}.

CONCLUSIONS

The drift capacity of flexural members is affected by the applied cyclic drift history, and it may be limited by sideways buckling of compression reinforcement in the plastic hinge regions. Upon cyclic strain reversals, the critical interaction diagram between strain ductility and the S_{st}/D_b ratio is mildly reduced due to stiffness degradation of the hysteretic loops, therefore and the value of $e_{sc,u}^{eff}$. The most dramatic influence is, however, the increase in residual strain owing to the pattern of displacement history cycles, leading to the conclusion that in members where bar buckling failure is a possible response mechanism (i.e. flexurally−dominant members), no dependable unique value of deformation capacity can be relied upon in either design or assessment, other than

lower bound estimates of this variable.

REFERENCES

Inel M., Aschheim M. and Pantazopoulou S. (2004), "Deformation Indices for Concrete Columns: Predicted vs. Measured", *13th World Conf. on Earthquake Engineering*, Vancouver, Canada, No 2397

Pantazopoulou S. J., (2003), Chapter 4 in "Seismic Assessment and Retrofit of R.C. Buildings", *fib Bulletin No. 24*, Case Postale 88, CH−1015, Lausane, Switzerland

Papia M., Russo G., Zingone G., (1988), "Instability of Longitudinal Bars in RC Columns", *ASCE, Journal of Structural Engineering*, **114:2**, 445–461

Pantazopoulou S. J. (1998), "Detailing for Reinforcement Stability in RC Members", *ASCE Journal of Structural Engineering*, **124:6**, 623−632

Ranf, R.T., Eberhard, M.O and Stanton, J.F. (2006), "Effects of Displacement History on Lightly Confined, R.C. Bridge Columns", *ACI Special Publication, SP−236*, 23−42

Syntzirma D., Thermou G., Pantazopoulou S., Halkitis G., (2006), "Experimental Research of R.C. Elements with Substandard Details", *1st European Conf. on Earthquake Engineering and Seismology*, Geneva, No 819

Syntzirma D., Pantazopoulou S. J. (2002), "Performance – Based Seismic Evaluation of R.C. Building Members", *12th European Conf. on Earthquake Engineering*, London, No 816

Zhu, L., Elwood, K. J., and Haukaas, T., (2006), "Assessment of expected failure mode for R.C. columns", *Proceedings of the 8th National Conference on Earthquake Engineering*, San Francisco, California

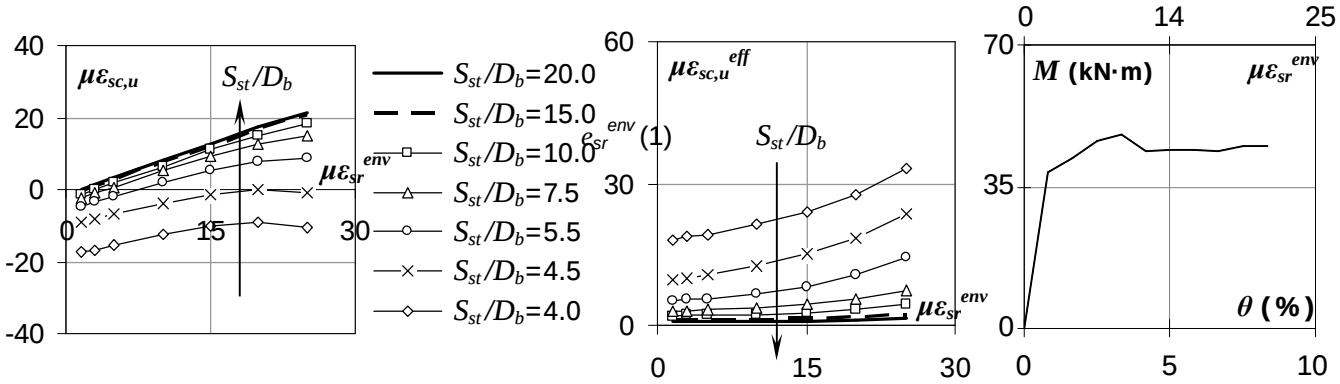

Figure 4 Example Case. Column with f_{sy}=400MPa, f_{su}=600MPa (e_{su}=0.05). Plot **(c)** results when the values of S_{st}/D_b=10.0, f'_c=20MPa and $f_b=0.5\sqrt{f'_c}$ are considered

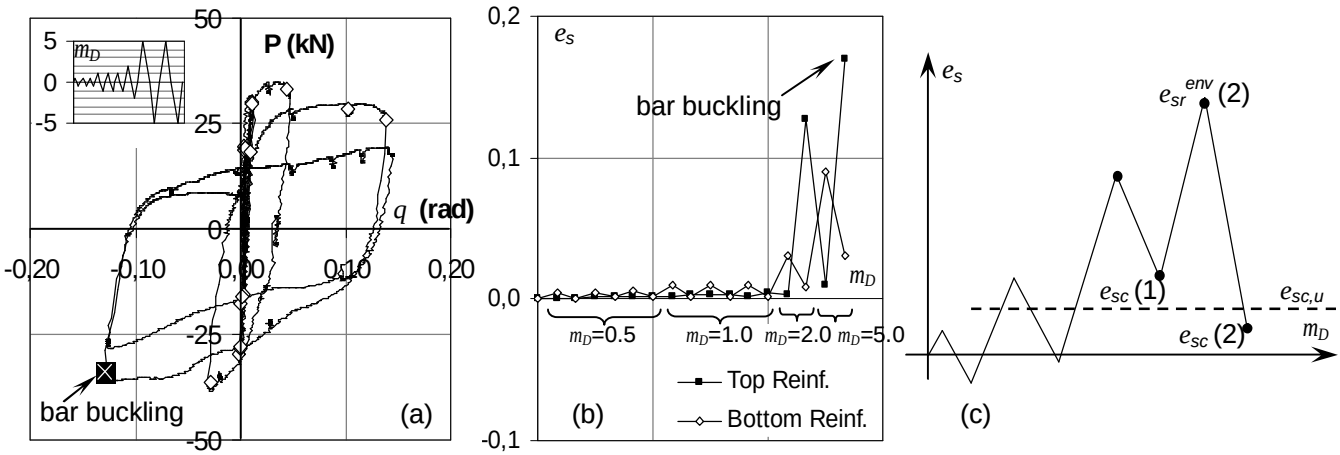

Figure 5 Response of a Prismatic Cantilever Column. **(a)** Load vs. Drift, **(b)** Strains in Top and Bottom Steel Layers. **(c)** Critical Strain $e_{sc,u}$ associated with Peak Tensile Strain attained in the Previous Step e_{sr}^{env}